Artificial neural network for modeling and prediction of selected dye removal and voltage generation from aqueous solution using microbial fuel cell

Nabea Muneer Mahdi, Ahmed Hassoon Ali*

College of Engineering, Department of Environmental Engineering, Mustansiriyah University, Iraq,
emails: env.eng.dr.ahmed@uomustansiriyah.edu.iq (A. Hassoon Ali), nb3mnr@gmail.com (N. Muneer Mahdi)

ABSTRACT

Microbial fuel cells (MFCs) are considered a low-cost engineered system and easy to construct. MFC was designed as a single-chamber, inoculation with activated sludge, and graphite plates as an electrode. A series of experiments were undertaken in a batch mode in MFCs, to access the effect of the process variable: pH, salt bridge type, molar concentration, temperature, dye concentration. The best parameters were found to be 7.5, KCl, 1.5 M, 30°C, and 500 mg/L where the maximum removal and voltage production was 70.3%, 822 mV, 74.7%, 994 mV, 80.8%, 1,395 mV, 85.7%, 1,989 mV and 93.8%, 2,800 mV, respectively. The batch experiment used adsorptive capacity for locally available and cheaper adsorbents: granite (G), porcelanite (PC), sawdust (SD), granular activated sludge, and groundnut shells (GS). Results showed that removal efficiency of adsorbents were in the consequence as: PC (69.3%) > GS (57.2%) > AS (52%) SD (43.8%) > G (24.3). Next experiments were focused on enhancing the performance of MFC by using the best adsorbents, Iraqi porcelanite show have good adsorption capacity dye, removal and voltage were obtained 95.8%, 2,789 mV. This study also investigates the removal of dyes (Congo red CR, Reactive black RB, Reactive yellow RY, and Methyl orange MO), decolorization of dyes was observed for the first at CR 98.6%, while in MO, RY, and RB is 96.2%, 91.5%, and 86.9%, respectively. In the terms of voltage, the maximum output voltage for CR, MO, RY, and RB is 2,877, 2,794, 2,574, and 2,454 mV, respectively. The artificial neural network model has been applied to accurately determine the most important factor in MFCs. It is observed that temperature plays a major role in decolorization and voltage production (100%) followed by a dye concentration of (84.3%).

Keywords: Microbial fuel cells; Dyes; Adsorbents; Microorganism; Decolorization; Bioelectricity

1. Introduction

Industries such as pharmaceutical, paper, food, and textiles use different kinds of dyes to color their products which creates one of the most detrimental problems of wastewater, as color is the foremost pollutant in the water to be recognized, thus most of the countries have mandated to decolorize the wastewater before its discharge into water bodies [1]. Especially, the textile industry is considered to have one of the most polluting wastewater effluents in the world, with regards to volume and composition, and large quantities of dyes used for coloring fabrics are present in the effluents. Dyes used in the textile industry generally consist of a group of atoms called chromophores, which are based on diverse functional groups such as azo, nitro, carbonyl, etc. About 200,000 tons of these dyes are lost to effluents in the textile industry every year, and azo dyes account for 60%–70% of dyes produced in the world. Their resistance to degradation damages the aesthetic quality and transparency of receiving water bodies [2].

Increasing the need for energy accompanied by a continuous depletion of fossil fuels not to mention its

* Corresponding author.

notorious environmental effects, scientists and researchers started looking for ways to harvest energy from renewable natural resources. These sources are typically inexhaustible on a human scale, sustainable, and offer a good alternative to the use of fossil fuels. The microbial fuel cell (MFC) is a promising clean energy source that has been the subject of active research since 1970 [3].

MFC is a novel and emerging technology for wastewater treatment. This system can convert organic pollutants present in wastewater to bioelectricity. The phenomenon that follows to generate electricity in the MFC is the bacterial cellular respiration through its metabolic activity attributed to converting organic substrate into electricity, which aids for wastewater treatment process [4]. MFC is a bio-electrochemical system that produces electric current from organic matter as the result of bacterial interaction [5,6]. Most MFC configurations contain; anodic and cathodic, separated by a membrane [7,8]. Oxidation takes place at the anode under anaerobic conditions due to the consumption of an organic substrate by microorganisms [9]. Electrons and protons are simultaneously generated in the anodic chamber and travel through the external circuit and proton exchange membrane, respectively, to the cathode where they are utilized in a reduction reaction Recently, a wide range of applications has been recognized with MFC frameworks like seawater desalination, hydrogen production, biosensor technology, and heavy metal and dye degradation [10].

Adsorption is carried out mostly by using activated carbon because of has high adsorptive capacities. But the production of activated carbon is expensive and its regeneration is very difficult [11]. Recent research has been directed towards looking for alternatives to investigate a low-cost method, which is both economical and effective and can be used on an industrial scale. Among the treatment technologies, biosorption is getting prominence because it is economically favorable, effective, and technically feasible [12].

Ali et al. [13] fabricated a conventional microbial fuel cell (CMFC) consisting of a single chamber used as an anode chamber with an agar-salt bridge pipe, graphite plate electrode, manciple wastewater (bacteria source and substrate), while modified MFC was designed. CMFC container was connected with screens and granular activated carbon (GAC) pipe, for removing nutrients and heavy metals from wastewater and for electricity generation The results showed that modified MFC had maximum removal

efficiencies for NO_3 (58.89%), PO_4 (74.98%), chemical oxygen demand (COD) (91.74%), total suspended solids (98.16%), Pb (91.39%) and Cu (92.78%), while CMFC removal efficiency found to be 51.865%, 66.03%, 85.267%, 83.22%, 58.91% and 61.66% for these parameters, respectively [13].

The purpose of this study is biodegradation of dye (substrate) from aqueous solution by designing single-chamber MFCs, using sludge (bacteria source), and finding optimization of the operational parameter such as pH, type of salt, molarity, temperature, different concentrations of dye, select the effective adsorbents, and study the effect of different type dyes on the performance of MFC in both power generation and decolorization, then applied artificial neural network (ANN) to predict the voltage generation from MFC and removal efficiency of dye then comparing it with the experimental work.

2. Materials and methods

2.1. Cell design

Air cathode BFCs were constructed from an anode chamber made of a plastic container, total volume 6 L (operating volume 5 L plus a 1 L headspace), the reaction inside the chamber was anaerobic. At high 1 cm from the bottom, this chamber is connected to salt bridge PVC pipe (Di 1.5 inch and length 5 in). The sample port was located on the high 4 cm from the other side of the container to take samples for a checkup. The electrodes used were two graphite plates with a total surface area of 38.5 cm^2 (L = 11 cm, W = 3.5 cm, and T = 1 cm), one electrode is located inside the chamber as an anode (no catalyst) and the other electrodes (cathode) are located at the end of the pipe. Prior to use electrodes, it was soaked in distilled water for 24 h and washed to ease attachment of microbes and electron transfer. To complete the electrical circuit; the insulated copper wire was used to link these electrodes are All MFCs operated in batch mode under the proper conditions for a long-term experiment (20 d). Fig. 1 illustrates a schematic diagram of MFC.

2.2. Preparation agar salt bridge pipe

Agar salt bridge plays a major role in the transport of H$^+$ ions that liberate during anaerobic digestion of wastewater and are used to maintain electrical neutrality within the
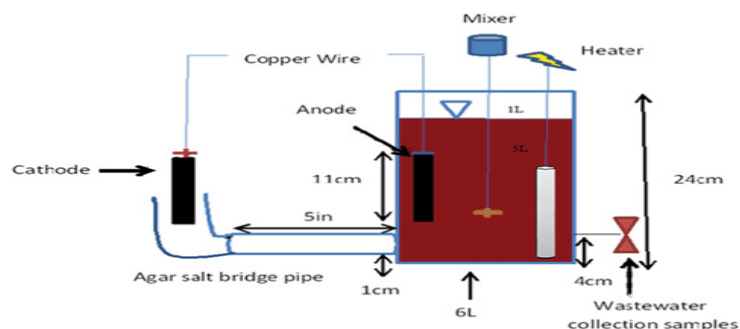

Fig. 1. Schematic diagram of SMFC.

internal circuit. Agar bacteriological was used as solid media. The salt bridge pipe was prepared by using 15% of agar dissolving in a solution that contains salt. The prepared solution from agar and salt was boiled and cast in the PVC pipe, then is stored in the refrigerator. Characteristics of agar are listed in Table 1.

2.3. Preparation of aqueous solution

The live activated sludge was kindly provided from Al Rustamiyah WWTP (the old project). It is located in Baghdad (33o16'30.8" N, 44o31'57.4" E). The media was prepared by dyeing Congo red dye in a conical flask with distilled water and put on stirred for total dissolution of the dye to get at a concentration of 200 mg/L, mixed with 2.343 g sucrose $C_{12}H_{22}O_{11}$ (468 mg COD/L) and 250 mL of sludge filter, before adding to media sludge was filtered by Whatman filter paper (Hardened Ashless, Grade 542, England) to remove impurities. The nutrient medium contained 7.75 g of ammonium chloride, and 3.25 g of potassium chloride was also added to the anode chamber. Table 2 shows the characteristic of Congo red (CR) dye.

2.4. Effect of pH

To study the effect of pH on voltage production and microorganism's growth, four OCMFC were operated at room temperature feed at the same time with the same substrate at different pH values (6.5, 7, 7.5, and 8). Sodium hydroxide (NaOH) and hydrochloric acid (HCl) were used for controlling the pH and using an agar salt bridge (15% agar + 1 M NaCl) to select the best pH to give maximum voltage and removal efficiency.
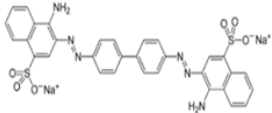
The decolorization and degradation of azo dyes under anaerobic conditions is a relatively simple and nonspecific

reduction process involving the azo reduction mechanism relying on redox intermediates. In direct enzymatic catalysis, non-specific azo reductase in microorganisms directly catalyzes the reduction of azo dye. However, the existence of this enzyme has not been directly verified. The reduction reaction relying on cofactors and redox mediators may be the main mechanism for the degradation of azo dyes under anaerobic conditions. At present, the main redox intermediates are FAD and NAD(P)H, etc. and they can receive electrons from an azo-reductase and then transfer the electrons to the azo dye. Then azo-bonds (–N=N–) are destroyed to produce aromatic amines, which decolorize the azo dye. The spontaneous

Table 1
Characteristics of agar

Item	Agar
Chemical name	Agar bacteriological, Pure, Agar-Agar
Molecular weight	336.337 g/mol
Chemical formula	$C_{14}H_{24}O_9$
Gel strength	700–1,000 g/cm³
Melting point	85°C–95°C
Viscosity	Low
pH	6–8

Table 2
Shows the characteristic of CR dye

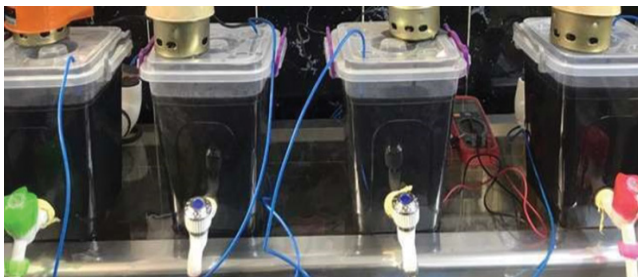| Item	Congo red (CR)
Trade name	Congo red
Wavelength (nm)	Solid/powder
Packing	500
Origin	England
Molecular formula	$C_{32}H_{22}N_6Na_2O_6S_2$
Molecular weight (g/mol)	696.6
Solubility	5 mg/mL
pH range	Blue (3.0) to red (5.0)
Chemical structure	

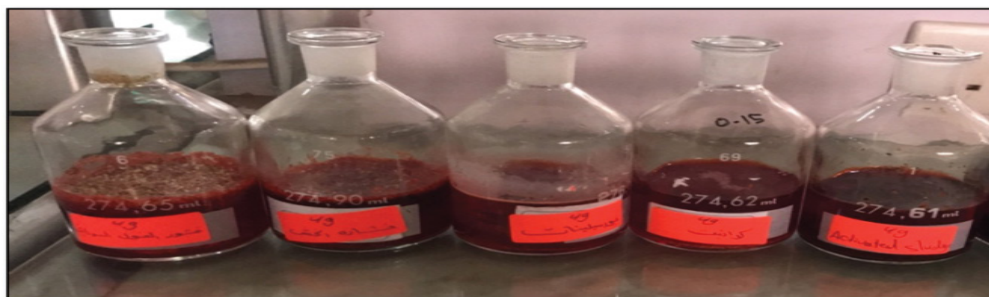Fig. 2. Four MFCs with different molar concentrations.

Fig. 3. The glass bottles contain CR (100 mL) with different adsorbents (5 g).

non-specific reduction reaction between the azo dye and redox intermediates mainly depends on the redox potential. According to related reports, under anaerobic conditions, the redox potential of 50 mV can lead to the effective decolorization of azo dyes. However, the cleavage of the chromophore groups of dyes results in colorless, odorless, and toxic intermediate metabolites of aromatic amines, which are commonly mineralized under aerobic conditions. Furthermore, it has been reported that the presence of oxygen usually suppresses the reduction activity of the azo bond because aerobic respiration may dominate the utilization of NADH and impede the transfer of electrons from NADH to the azo bond. It has also been reported that aromatic amines containing functional hydroxyls and carboxyl groups can be mineralized under anaerobic conditions. Some aromatic amines which are prone to undergo self-oxidation can be degraded under anaerobic conditions. Menek and Karaman [14] stating that the –N=N– azo bond reduced to hydrazo (I) or amine (II), by consuming two or four electro.

$$-N = N - +2e + 2H^+ \rightarrow -NH - NH - \tag{I}$$

$$-N = N - +4e + 4H^+ \rightarrow -NH_2 - NH_2 - \tag{II}$$
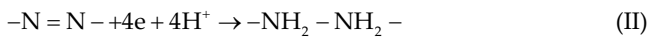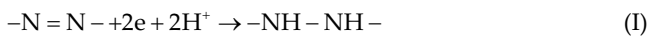
2.5. Agar salt bridge type

Two MFCs were operated at the same time and fed with the same substrate to choose the best agar salt bridge type (i.e., KCl or NaCl) on the bacterial fuel cells. One cell used a NaCl salt bridge and the other operated with KCl. The concentration of NaCl and KCl was fixed at 1 M and 15% of agar, the system was maintained at room temperature, and depending on voltage and removal efficiency choose the better salt bridge type (i.e., either KCl or NaCl).

2.6. Salt bridge molar concentration

Varied salt concentrations (0.5 M, 1 M, 1.5 M, and 2 M) were used to prepare four agar salt bridge pipes in a novel

BFC design were analyzed. Four AC-BFCs were fabricated to study the effect of the molar concentration shown in Fig. 4; agar salt bridge type was obtained from the previous experiment. The cells were operated at the same time with a similar aqueous solution. The voltage production was measured with time, check samples, and the molar concentration that gives maximum removal efficiency and voltage production will be used in further experiments. Fig. 2 shows four MFCs with different molar concentrations.

2.7. Effect of temperature

To study the effect of temperature on bacteria activity, four AC-BFCs are built and operating at the same substrate with different temperature degrees (25°C, 30°C, 35°C, and 40°C) using an electrical heater with a thermostat, the best agar salt bridge type, and molar concentration was kept from the previous experiments. Depending on maximum voltage output and high removal efficiency choose the best temperature.

2.8. Effect of dye concentration

To explore the effect of CR dye concentration, MFCs were charged with different CR dye concentrations (100, 200, 300, and 500 mg/L) in the anodic chamber and observed effects on voltage and removal. pH, type of salt, molarity was kept at the best value obtained from previous experiments.

2.9. Batch experiment

In order to select the best adsorbent from granite (G), porcelanite (PC), sawdust (SD), granular activated sludge (GAS), and groundnut shells (GS) in removing CR from aqueous solution. Five glass bottles of the volume contain 100 mL solution of initial concentration 100 mg/L, the. The dose of each adsorbent was 5 g, as shown in Fig. 3. The glass bottles were then placed on a shaker (Heidolph Unimax) and agitated continuously for 3 h at 250 rpm. The samples were filtered by Whatman filter paper then measured by means of a spectrophotometer device to measure absorbance, then calculated removal efficiency
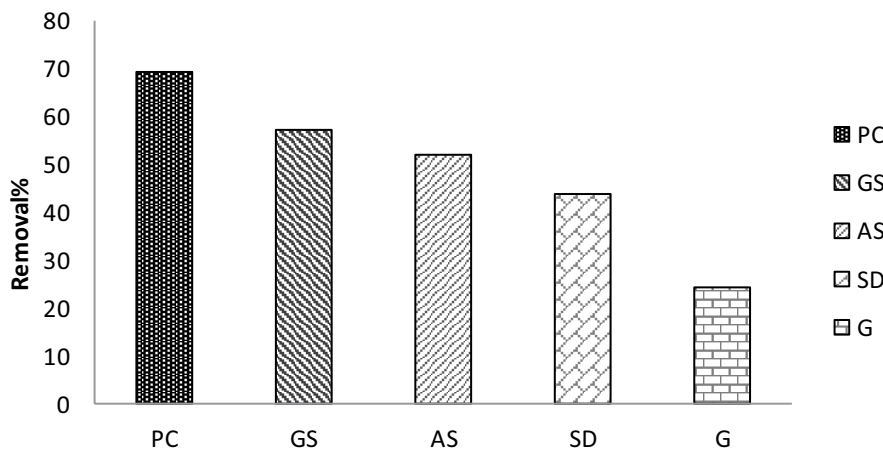

Fig. 4. The removal efficiency of CR onto different adsorbents.

by Eq. (1). The results are shown in Fig. 4. It can be seen that the dyes removal efficiency by PC is greater than those by other adsorbents. The arrangements of adsorbents as a function of dye removal efficiency are as follows:

$$PC > GS > SD > GAC > G \qquad (III)$$

2.10. Preparation of adsorbents

2.10.1. Porcelanite

Porcelanite is a term used by Iraqi Geologists to identify siliceous rock resembling diatomite. Porcelanites are composed of opal-CT (cristobalite-tridymite crystal stratification) derived from biogenic amorphous opal silica (mainly from diatoms). PC which is a natural sorbent has been brought from the Iraqi Ministry of Industry, Geological Survey Department. PC was broken manually, grinding, and sieved. The PC was washed with distilled water to remove any non-adhesive impurities and small particles and left to dry completely in oven-dried at 105 for 3 h and then again dried in sunlight for 6–8 h. The chemical characteristics of sorbent were taken from the Geological Survey Department are shown in Table 3. The PC was sieved into mesh 0.6, 1 mm using German sieves. For non-spherical particles, the particle diameter is defined as the equivalent diameter of a spherical particle with the same volume. As an approximation, the particle diameter may be calculated from the geometric mean of the two consecutive sieve openings without introducing serious errors. The geometric mean diameter is given by, $d_{gm} = (d_1 d_2)^{1/2}$, where d_1 is the diameter of the lower sieve on which the particles are retained and d_2 is the diameter of the upper sieve through which the particles pass [15]. Fig. 5 shows the prepared porcelanite.

2.10.2. Granular activated sludge

The steps in the preparation of GAS are as follows [16]:

- Drying of anaerobic sludge at dry climate conditions (temperature at 303 ± 5 K and relative humidity of 45%) for 2 d.
- Formation of the flocks of dried dead anaerobic sludge.
- Grinding the flocks using agate mortar.
- Sieving the resulting biosorbent by the same sieves as in PC.
- The GAS was washed thoroughly using distilled water to remove any coarse impurities.
- After washing, GAS was dried using the electric oven for 24 h at 333 K to avoid the alteration of functional groups. Fig. 6 shows the prepared granular activated sludge.

2.10.3. Groundnut shells

Process of activation: firstly, GS grinding and sieving result in the same sieves as in PC. Then unwanted material (suspended impurities) like salt, dust, etc. were removed by extensively washing in running tap water for removing. It was followed by washing with distilled water. The washed

Fig. 5. Porcelinite before and after cracking.

Fig. 6. Anaerobic sludge during drying, flocks of drying dead anaerobic sludge, and after grinding.

material was oven-dried at 105°C for 3 h, the biosorbent was ready. Fig. 7 shows the prepared groundnut shells.

2.10.4. Sawdust

The sawdust was collected from several furniture factories in Baghdad where large amounts are produced as residuals from the production of different furniture. This was washed with double distilled water to remove water-soluble impurities and surface adhered particles. Then the adsorbent was oven-dried at 105°C for 3 h to remove the moisture and other volatile impurities. Fig. 8 shows the prepared sawdust.

2.11. Effect of adsorbents

After a batch test, the four best adsorbents were selected then based on four MFCs to study the effect on voltage, removal, and time, after keeping the best pH, type of salt, molarity of salt, and dye concentration. 30 g of adsorbent with electrodes packed in cylindrical stainless steel cages (mesh ≅0, radius = 1 cm and high 12 cm). Fig. 9 shows the stainless cages.

2.12. Effect of dyes type

At the optimum conduction, four different dyes (Congo red (CR), Methyl orange (MO), Reactive black (RB), and

Reactive yellow (RY)) were used to appear that different dyes could be decolorized to various extents. Dyes dissolved in distilled water that contains the best concentration obtained from previous experiments were put on stirred for total dissolution of the dye. Table 4 shows the specifications of these dyes . Fig. 10 shows the MFCs with different dyes (RY, MO, RB, and CR).

2.13. Analysis

The voltage was measured in an open circuit every day using digital a multimeter (UNI-T model) for 20 d. The maximum wavelength of (CR, RY, RB, and MO) dyes was specified using UV-VIS spectroscopy (Thermo Genesys 10 UV, USA) in the range of (400–800 nm) the highest absorbance for the dye was found by the calibration curve 500, 503, 651, and 533 nm, respectively. All the absorbance measurements were carried out as the respective wavelength max values to attain the maximum sensitivity of the instrument. Initially, before checkup, collected samples were filtered through Whatman filter paper (Hardened Ashless, Grade 542, England) to remove any particulate matter. Fig. 11 shows the samples filter for a check-up.

Decolorization is determined by the following equation:

$$\text{Dec.}\% = \left(\frac{C_1 - C_2}{C_1} \right) \times 100 \tag{1}$$

where C_1 is the initial absorbance; C_2 is the observed absorbance.

2.14. Artificial neural network

ANN was applied to predict the effect of pH, molarity concentration of salt, temperature, and dye concentration on voltage production and removal efficiency. The experimental

Table 3
Chemical characteristics of PC (State Company of Geological Survey and Mining, Mining Center)

Sample No.	PC
CaO%	11.55
SiO$_2$%	62.02
Al$_2$O$_3$%	2.71
Fe$_2$O$_3$%	0.87
MgO%	7.2

Table 4
Characteristic of dyes
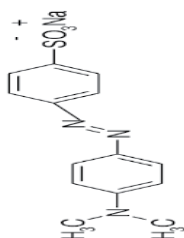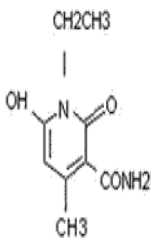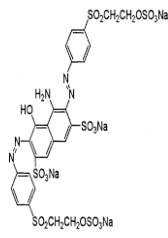
Item	Methyl orange (MO)	Reactive yellow (RY)	Reactive black (RB)
Trade name	Methyl orange	Cibacron yellow FN-2R	Cibacron black wnn-2R or Remazol Black B
Phase	Solid/powder	Solid/powder	Solid/powder
Wavelength (nm)	533	503	651
Origin	England	Swiss	Swiss
Molecular formula	$C_{14}H_{14}N_3NaO_3S$	$C_9H_{12}N_2O_3$	$C_{26}H_{21}N_5O_{19}S_6Na_4$
Molecular weight (g/mol)	327.33	176	991.8
pH	Red (2.9) to orange (4.6)	5.5–6	5.8
Solubility (mg/mL)	5	130	550
Chemical structure			

Fig. 7. Groundnut shells before and after grinding.

Fig. 8. Sawdust during sieve and after.

result data were used to carry out this modeling practice. The modeling was carried out using an artificial neural network-based IBM SPSS version 23.0 computer program.

The most important factors that are needed to be addressed in ANNs modeling include [17]:

- Determination of model inputs.
- Determination of model architect.
- Determination of modal optimization (training).
- Determination of stopping criteria and model validation.

3. Result

3.1. Effect of pH

Based on the experiment, the data collected shows that the effectiveness of the degradation increases around pH 7.5± removal efficiency, and voltage generation was obtained to be 70.3% and 822 mV, while in the pH 8, 7, and 6.5, the removal was 61.1%, 50%, and 38% and for voltage 690, 412, and 213 mV, respectively. The pH plays a major role in the efficiency of dye decolorization as it was associated with the overall biochemical processes and the growth of microbes. It was considered as another limiting factor for microbial activities and dye degradation.
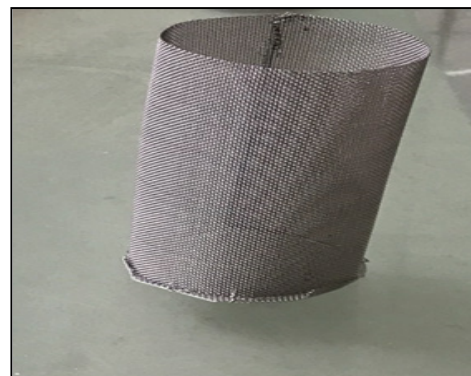

Fig. 9. Stainless cages.

Generally, the pH for color removal by bacteria often exists between 6.0 and 10.0 with good efficiency, Figs. 12 and 13 illustrate removal efficiency and voltage production at different pH within 20 d [18]. The majority of the azo dye reducing bacterial species were able to decrease the dye at a pH near 7.5. This may be related to the transport of dye molecules across the cell membrane [19]. Also, in the beginning, at the anode compartment, the pH value
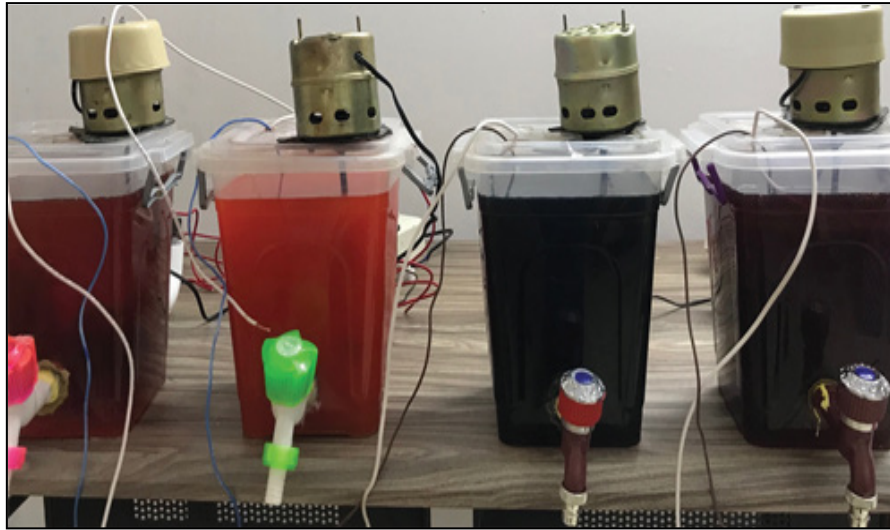
Fig. 10. MFCs with different dyes (RY, MO, RB, and CR).

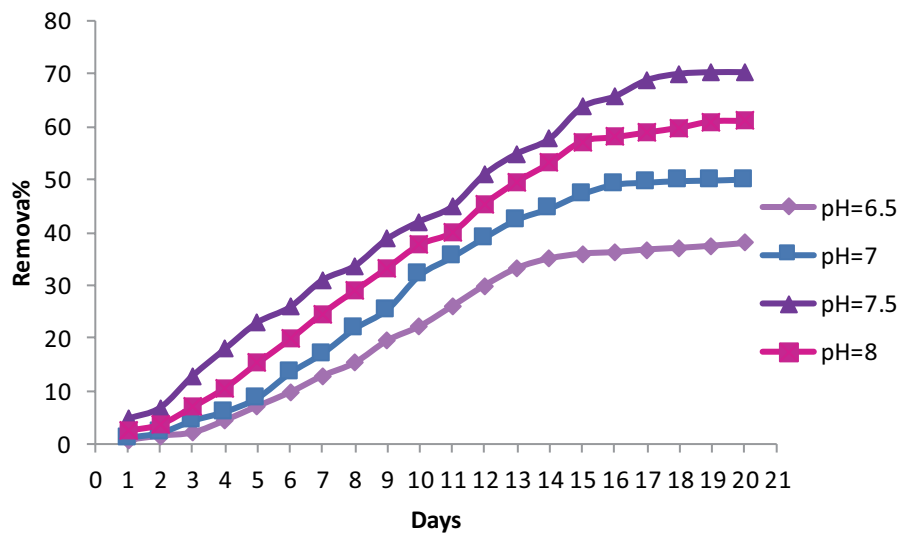Fig. 11. Shows the samples filter for a check-up.

Fig. 12. Decolorization efficiency at different pH.

decreases due to proton generation and then increases gradually because of the high current generation because more H^{+} ions are utilized in the cathode by the catholyte, so the anode compartment becomes more acidic. After a period, remains stable, because of the constant passage of H^{+} ions and the high current production. Finally, the anode compartment becomes acidic because of substrate degradation and the slow production of H^{+} ions [20].

3.2. Effect of salt bridge type

Two strong salts were used to prepare agar salt bridge pipes and were tested and compared to choose the best salt, potassium chloride (KCl) and sodium chloride (NaCl). As is clear from Figs. 14 and 15, there was no match difference in the result. The maximum removal efficiency and voltage output obtained from 1 M KCl and 1 M NaCl were 74.7%, 994 mV, 70%, and 830 mV, respectively, as shown in Fig. 14. It was found that KCl is better than NaCl. This

may be attributed to that; the transport number of sodium ions in pure water is about 0.4 while the transport number of potassium ions is about 0.49 [21]. NaCl may cause an imbalance of ions in the electrochemical cell, while KCl is very soluble so, it provides more positive K^{+} ions and negative Cl^{−} ions in solution and this will enhance the generation of the voltage. These results agree with those obtained by others [22]. Thus, KCl will be used in further experiments.

3.3. Effect of molar concentration

The effect of molar concentrations on removal and voltage is shown in Figs. 16 and 17. The study shows the interdependencies that exist among the effect of molarity concentration of salt bridge pipe in MFCs on dye removal and electricity output. The maximum removal and voltage obtained from 0.5, 1, 1.5, and 2M KCl was found to be 61.7%, 809 mV, 75.1%, 1,017 mV, 80.8%, 1,395 mV, and
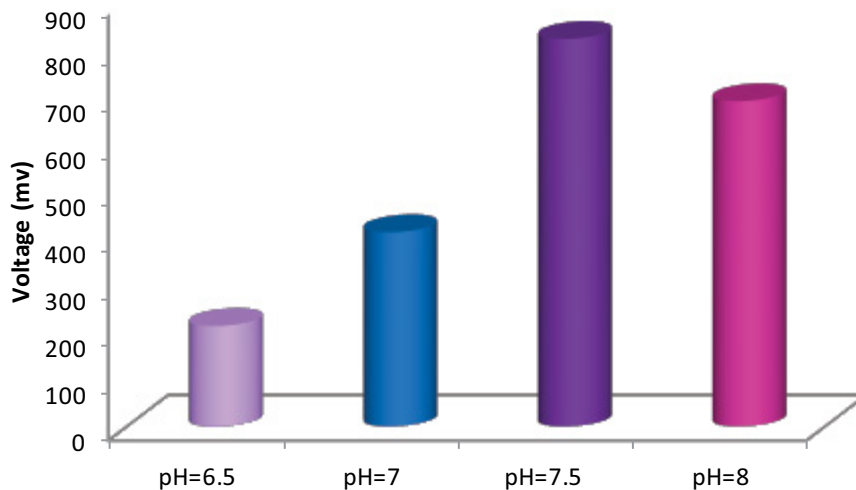

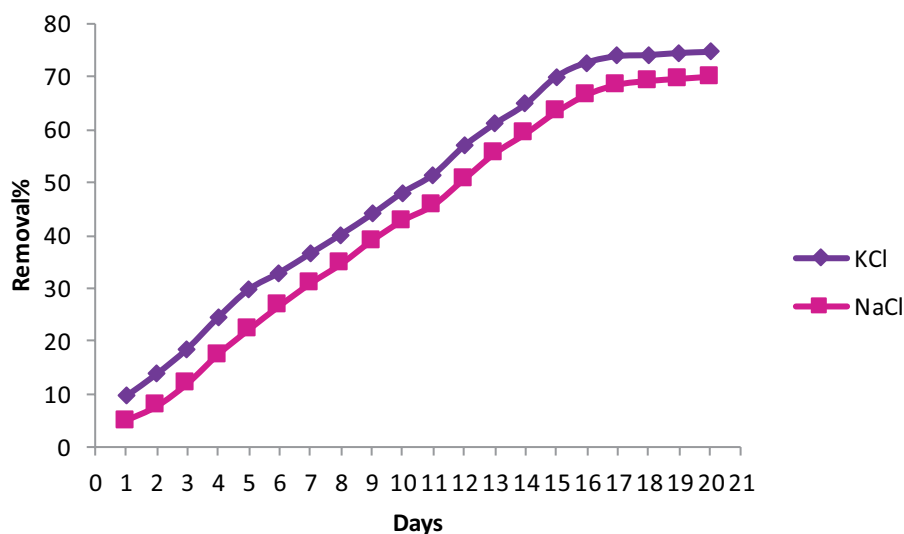Fig. 13. Output voltage (mV) through 20 d.

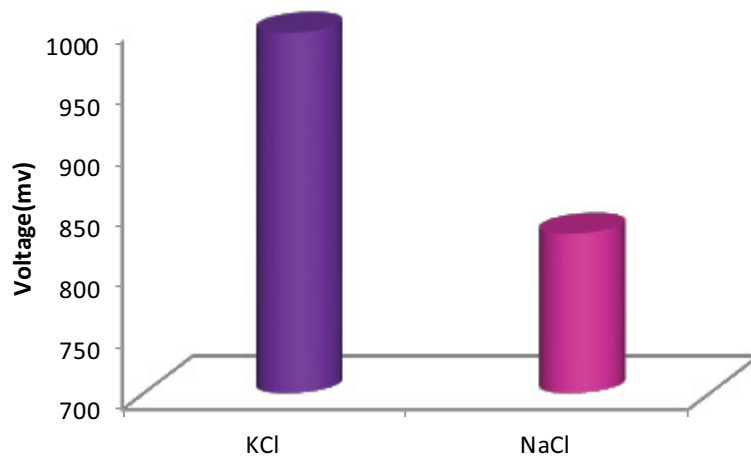Fig. 14. Decolorization efficiency at different salt bridge types.

Fig. 15. Voltage per day changes according to plant species at 1 am.
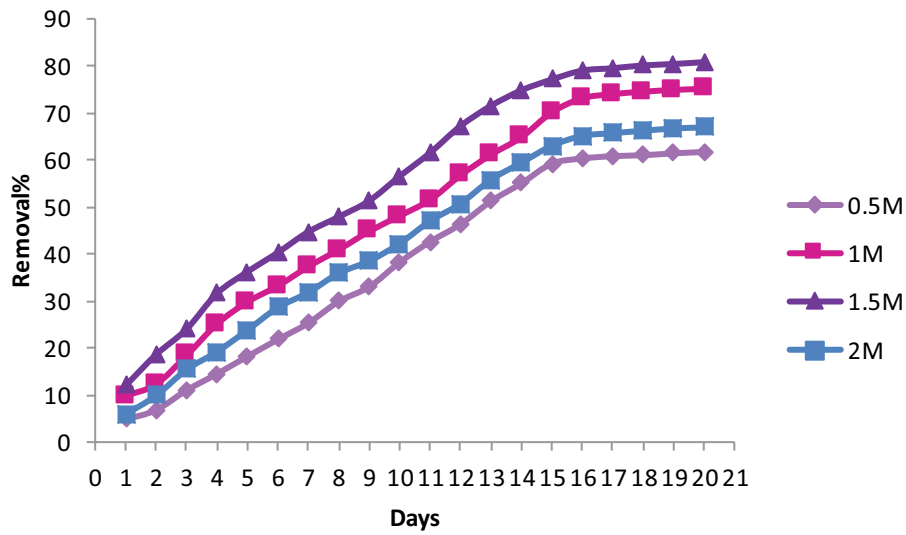

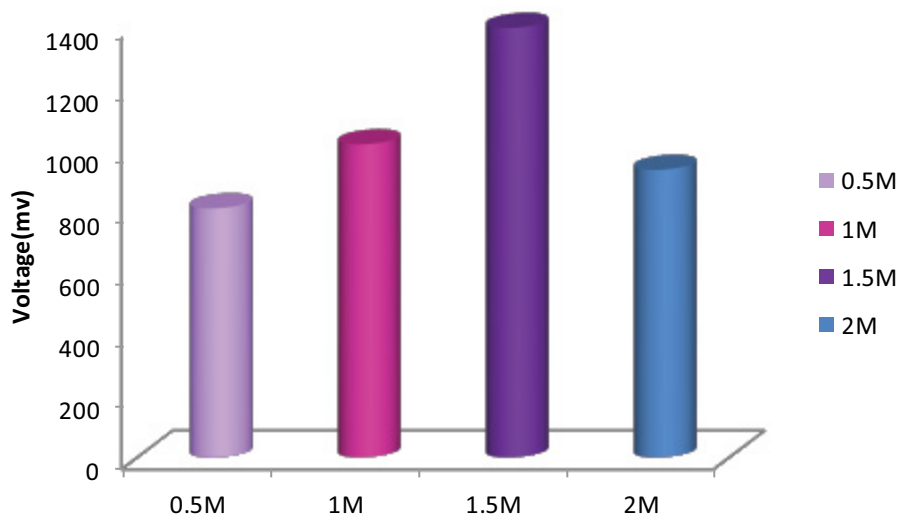Fig. 16. Decolorization efficiency at different molar salt concentrations.

Fig. 17. Output voltage (mV) through 20 d.

66.9%, 934 mV, respectively. Observed through 20 d of operation in batch mode, the removal efficiency and voltage of cells operated in 1.5 M, greater than cells operated in 0.5, 1 M, and 2 M. The molar concentration of salt is critical; since the transfer of protons through the salt bridge is facilitated by the dissociated ions in it and also salt decreases the activation loss. Min et al. [23] used salt bridge in MFCs with pure culture (G.metallireducens/m^2), obtained an average power density of (0.3 mW) and this power production was smaller than that achieved with the mixed culture used in this study.

3.4. Effect of temperature

The four cells operated at different temperatures (25°C, 30°C, 35°C, and 40°C) at the best conditions obtained previously. The optimum temperature degree for microbes gives maximum metabolic activities Congo red decolorization

and maximum voltage production is 30 ± °C were obtained to be 1,989 mV and 85.7%, respectively. For temperatures values of 25°C, 35°C, and 40°C, the maximum voltage production was 1,399, 1,648, and 780 mV and for removal 81%, 71%, and 64.7%, respectively are shown in Figs. 18 and 20. It was found that the performance of the anode enhanced with increasing temperature also enhances the oxygen reduction kinetics and decreases the internal resistance of the cell, which can lead to greater current densities and greater Columbia efficiency [24].

Higher or lower temperatures would inhibit cell viability, electron transport capacity, decomposition of biofilm, inactivation of bacterial metabolic activities, and putative enzyme activity responsible for dye reduction. In addition, the biodegradation activities by bacteria were affected by changes in temperature. According to a study conducted by [25], it was found that in microbial physiology, temperature changes lead to a sudden alteration of the activation
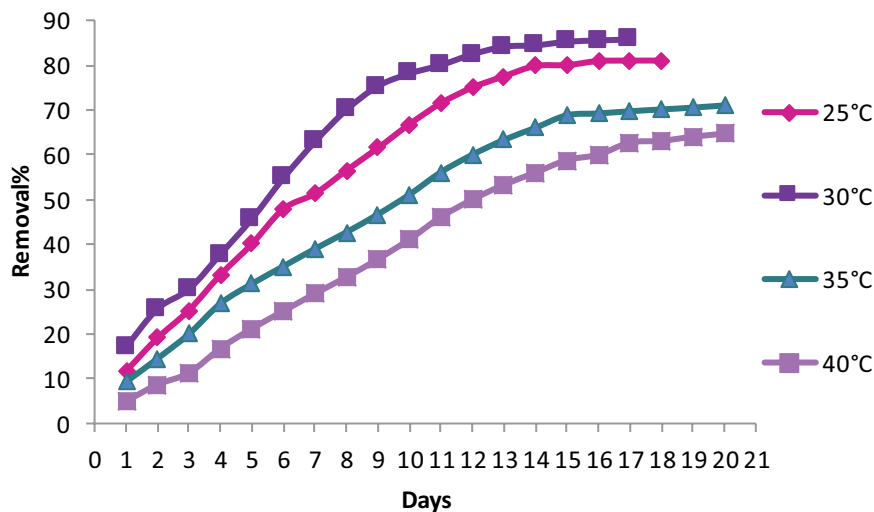

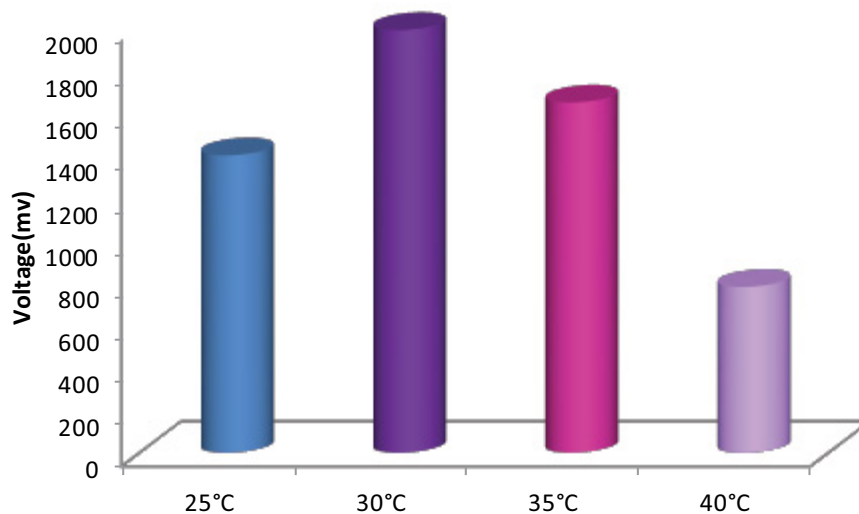Fig. 18. Decolorization efficiency at different temperatures.

Fig. 19. Output voltage (mV) through 20 d.

energy. Furthermore, further increase in the temperature may decrease the percentage of degradation. This phenomenon might be caused by the loss of cell viability or the denaturation of the azo reductase enzyme secretion at higher temperatures [26]. It is also likely that bacteria were mesophilic bacteria because they showed better decolorization in the temperature range of 25°C–35°C.

3.5. Effect of dye concentration

To explore the effect of CR dye concentration, MFC was operated with different CR dye concentrations (100, 200, 300, and 500 mg/L) in the anodic chamber. Figs. 20 and 21 show the effect of initial CR dye concentration on the removal and output voltage. It was observed that the rate of decolorization increased with increasing dye concentration reach 93.8% at 500 mg/L in interval time 15 d

where at concentrations 300, 200, and 100 mg/L, the removal reached 89.2%, 86%, and 65.7% respectively at time longer from 500 mg/L. In terms of voltage, the maximum voltage for dye concentrations 100, 200, 300, and 500 mg/L is 1,410, 1,991, 2,289, and 2,800 mV respectively. The sharp decline in the voltage is due to the low electron generation, which is directly proportional to the COD of the anolyte. 100 mg/L CR contains low organic carbon content, which reduces the oxidation activity of microorganisms [27,28]. Thus, the favorite concentration for the bacteria in the mixed culture was found to be 500 mg/L for the given conditions.

3.6. Effect of adsorbent

An adsorbent is expected to have high selectivity, high adsorption capacity, and long life. Furthermore, an adsorbent should be available in abundance at economical
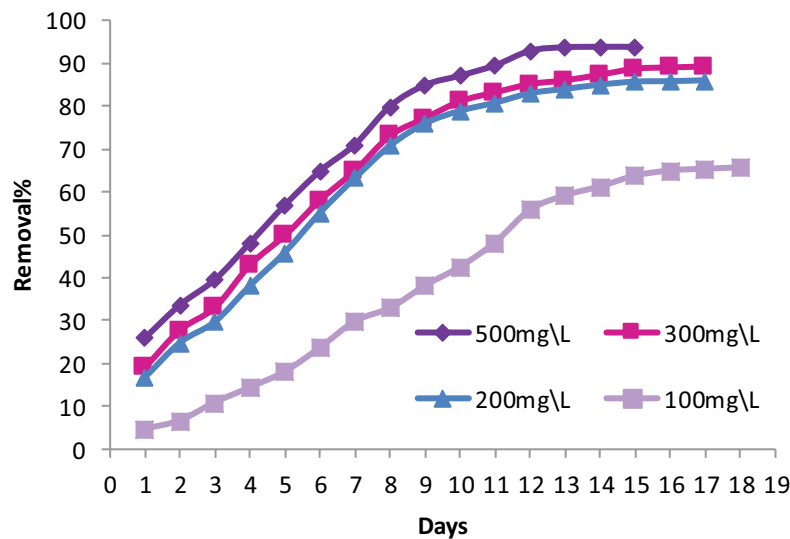

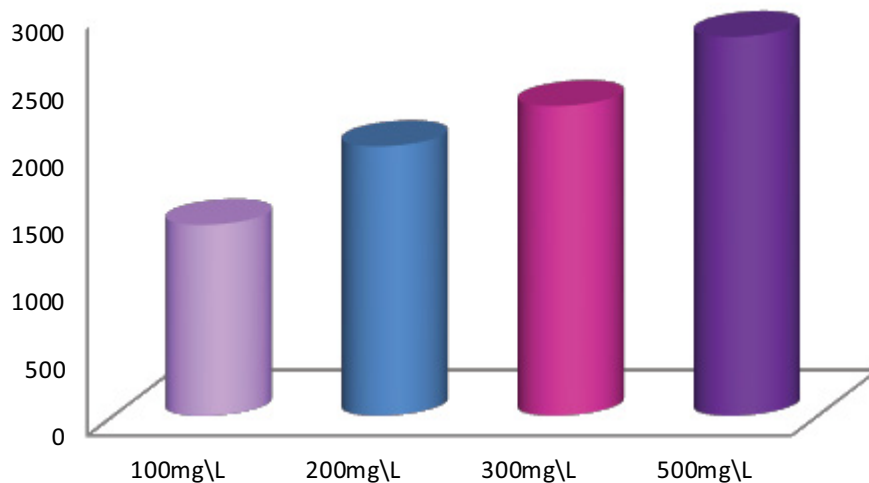Fig. 20. Decolorization efficiency at different dye concentrations.

Fig. 21. Output voltage (mV) through 20 d.

costs [29]. A wide variety of adsorbents is commercially available. Based on the experiment, the best adsorbent from GAC, PC, GS, and SD arrangements are as follows:

$$PC > GS > GAC > SD \qquad (IV)$$

The maximum removal efficiency and voltage production obtained to be 95.8%, 2,789 mV, 93% 2,592 mV, 92%, 2,488 mV, and 90%, 2,340 mV, respectively, the results are shown in Figs. 22 and 23. It can be seen that the dye removal efficiency by PC is greater than those by other adsorbents. This behavior may be attributed to The Iraqi porcelain rocks containing high levels of silicon up to 50% [30].

3.7. Effect of dyes type

Decolorization of dyes CR, RB, RY, and MO was observed for the first at CR 98.6%, while in MO, RY, and RB is 96.2%, 91.5%, and 86.9%, respectively. In the terms

of voltage, the maximum output voltage for CR, MO, RY, and RB is 2,877, 2,794, 2,574, and 2,454 mV, respectively. This is due to the dye that has a low solubility value being faster to remove. Many researchers had studied the performance of different MFC modes, including single chamber (SCMFC) and dual-chamber (DCMFC), to treat dyes contaminated wastewater and for voltage production under different circumstances [31,32]

3.8. Applying artificial neural network

For predicting the most important factor effect on voltage and removal, the used network architecture is illustrated in Fig. 26 which consists of four input neurons corresponding to the state variables of the system, with one hidden neuron and two output neurons. All neurons in each layer were fully linked with the neurons in an adjacent layer. The light and dark color lines linking between layers and neurons in the architect structure represent the significance of the connecting weights. The figure also
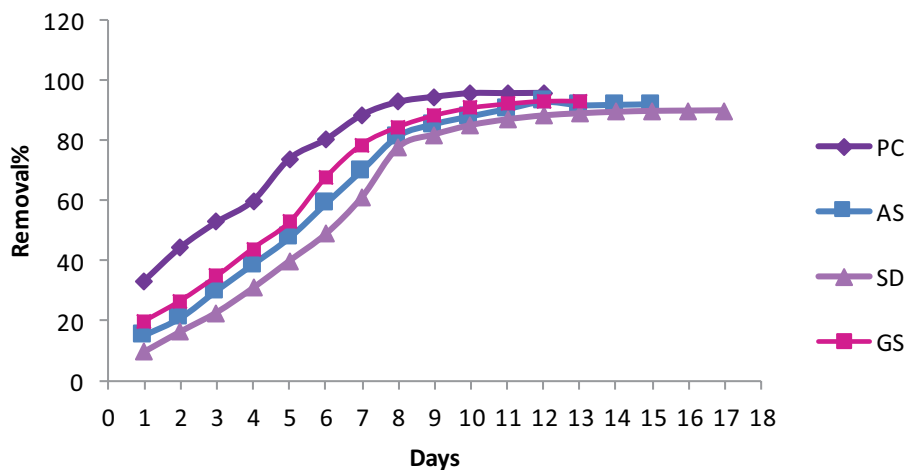

Fig. 22. Decolorization efficiency at different adsorbents.
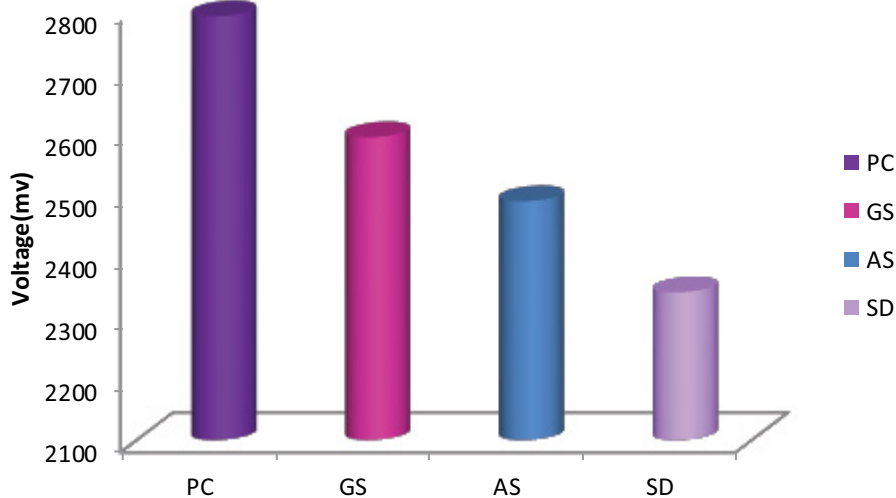

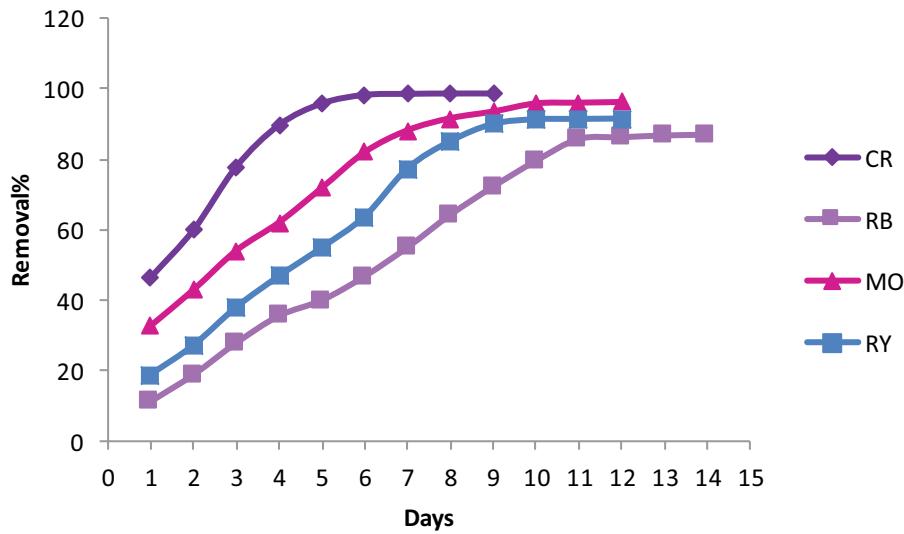Fig. 23. Output voltage (mV) through 20 d.

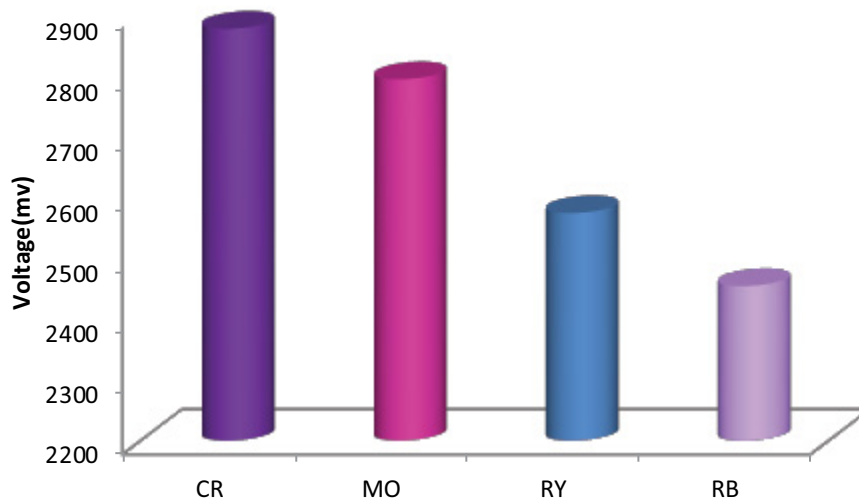Fig. 24. Decolorization efficiency at different dyes type.

Fig. 25. Output voltage (mV) through 20 d.

shows the type of activation function that bonds between the input and hidden layer (hyperbolic tangent) and the activation function between the hidden and output layer (identity). Table 5 shows the details of the model network information.

The estimated parameters for the input and output layer with their corresponding biases that were obtained from the SPSS model program are shown in Table 6. In this table, the value of the weights from the input to the hidden layer and from the hidden layer to the output layer is also shown.

The importance of the independent variable (inputs) which is a measure of how much the network's model predicts output voltage changes for different values of the independent variables is shown in Fig. 27. It is observed that temperature plays a major role in voltage production and removal (100%) followed by the dye concentrations at importance of 84.3% as shown in Table 7.

3.9. Appling multiple correlation equation (MCE)

The multiple correlation methodology was employed to determine the relationship between operating parameters (pH, molar concentration of salt bridge pipe, temperature, and dye concentration) and removal/voltage generation. Equation ($Y = aX_1bX_2cX_3dX_4e$) was solved to determine these relationships by the application of the Excel program.

Based on the experimental data, the independent variable coefficient can be calculated. The correlation coefficient (R^2) is close to 1, which indicates a good correlation between the experimental and predicted values. Table 8 shows a reprehensive equation for best removal efficiency for dyes and voltage generation and its correlation coefficient. The maximum voltage generation in experimentally obtained at best conditions which are (pH 7.5, 1.5 M KCl, 30°C, and 500 mg/L) respectively, is close to that determined from multiple correlations.
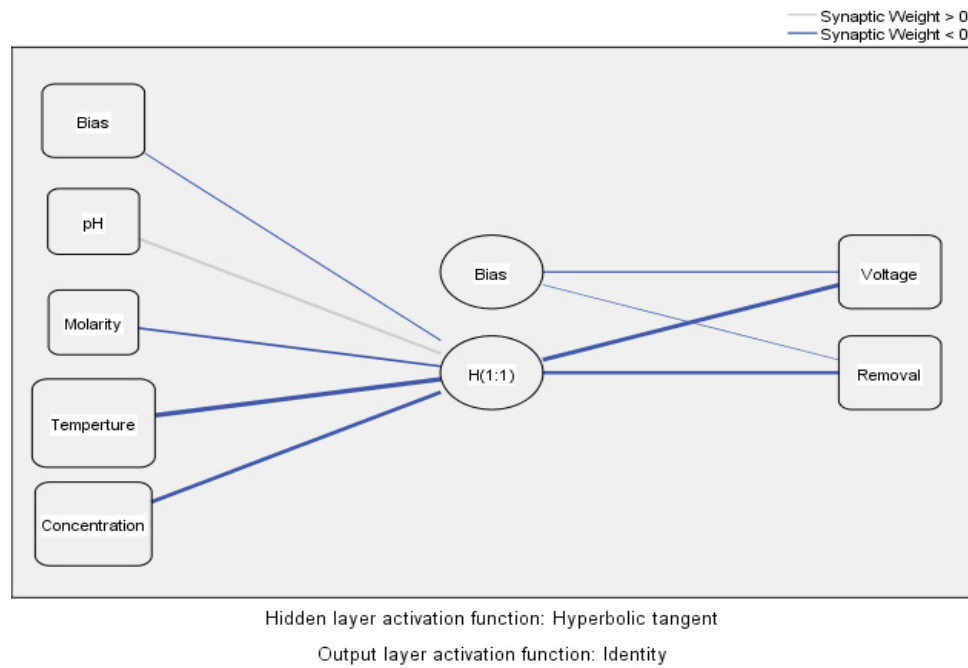
Fig. 26. Structure of a layer neural network.

Table 5
Artificial neural network information

Network information			
Input layer	Covariates	1	pH
		2	Molarity
		3	Temperature
		4	Concentration
	Number of units[a]		4
	Rescaling method for covariates		Standardized
Hidden layer(s)	Number of hidden layers		1
	Number of units in hidden layer 1[a]		1
	Activation function		Hyperbolic tangent
Output layer	Dependent variables	1	Voltage
		2	Removal
	Number of units		2
	Rescaling method for scale dependents		Standardized
	Activation function		Identity
	Error function		Sum of squares
[a]Excluding the bias unit			

3.10. Mechanism of dye removal and bacterial growth patterns

The bacterial growth started to increase gradually at first (lag phase), then increased rapidly until it reaches a maximum (log phase), then the increase becomes steady due to substrate decreasing for metabolic processes. The dye removal and voltage generation are high on the Log phase and then become steadily at a stationary phase which proves the relationship between dye concentration (substrate) and bacterial activity and voltage generation. Fig. 28 shows the bacteria growth pattern [33].

4. Conclusions

The study showed a number of conclusions during batch mode and under anaerobic experiments for decolorization dyes and bioelectricity generation:

Table 6
Model parameters estimates for voltage and removal

Parameter estimates		Predicted		
		Hidden layer 1	Output layer	
Predictor		H(1:1)	Voltage	Removal
Input layer	(Bias)	–0.106		
	pH	0.237		
	Molarity	–0.136		
	Temperature	–0.945		
	Concentration	–0.607		
Hidden layer 1	(Bias)		–0.114	–0.091
	H(1:1)		–0.647	–0.555

Table 7
Independent variable importance

Independent variable importance		
	Importance	Normalized importance
pH	0.102	23.1%
Molarity	0.085	19.4%
Temperature	0.441	100.0%
Concentration	0.372	84.3%

- Microbial fuel cells show good performance by constricted simplest design with local materials.
- Using activated sludge is preferred as a vital source for treatment, saving energy, and cost-effectiveness.
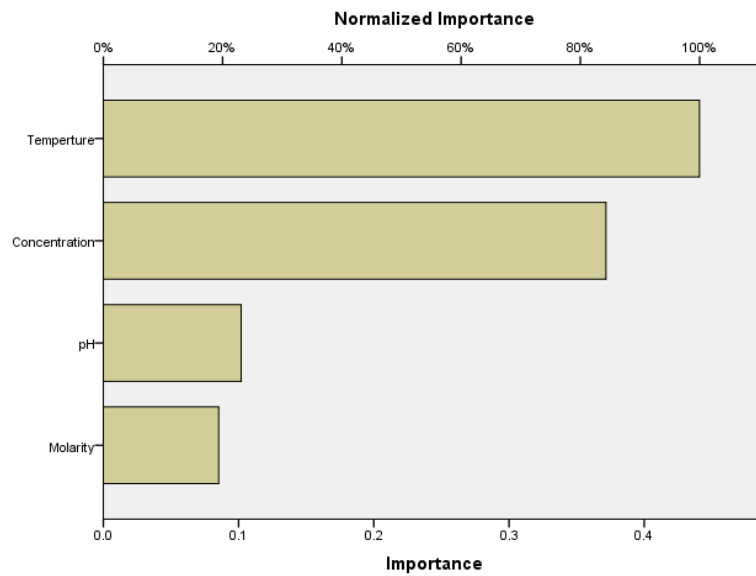- With the experimental data obtained in this study, it is

Fig. 27. Independence variable importance of molarity and temperature estimated by ANN.
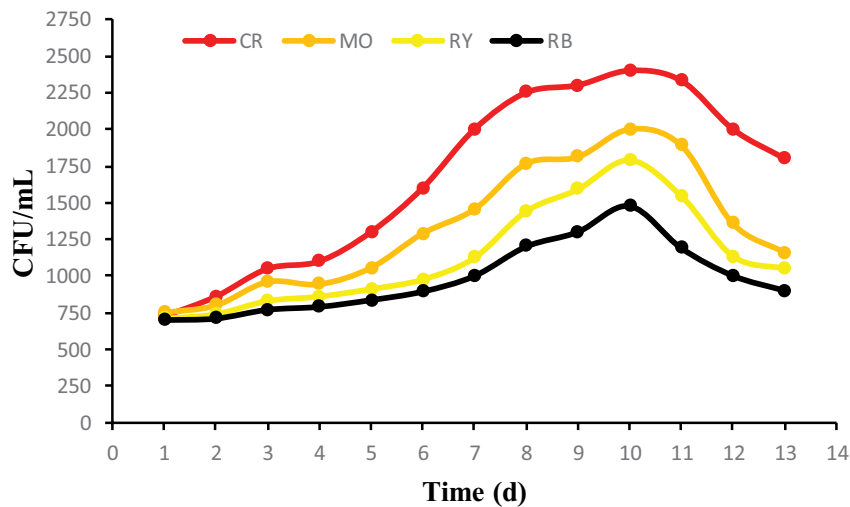

Fig. 28. Bacterial growth pattern at four dyes MFC systems.

Table 8
Reprehensive equation for best removal efficiency for dyes and voltage generation and its correlation coefficient

R^2	Equation	$Y_{practical}$	$Y_{theoretical}$
99.17	$Y = 0.997\,(X_1^{1.35573} \times X_2^{0.36110} \times X_3^{0.14927} \times X_4^{0.17028}$	93.8%	84%
99.44	$Y = 0.993\,(X_1^{-0.09615} \times X_2^{0.73737} \times X_3^{1.12648} \times X_4^{0.60431}$	2,672 mV	2,160 mV

possible to design and optimize an economical treatment process for dyes removal and sustain high power generation.
• Adsorbents are normally used for their environmental-friendly behavior, availability in nature, and are very much cost-effective. So, it can be substituted for expensive activated carbon.

Acknowledgment

References

[1] P.L. Meena, Green materials for removal of dyes present in wastewater, Int. J. Sci. Eng. Res., 5 (2014) 5–7.
[2] F.M.D. Chequer, G.A.R. de Oliveira, E.R.A. Ferraz, J. Carvalho Cardoso, M.V.B. Zanoni, D.P. de Oliveira, Textile Dyes: Dyeing Process and Environmental Impact, M. Günay, Ed., Eco-Friendly Textile Dyeing and Finishing, InTechOpen, January 2013.
[3] M.H. Do, H.H. Ngo, W.S. Guo, Y. Liu, S.W. Chang, D.D. Nguyen, L.D. Nghiem, B.J. Ni, Challenges in the application of microbial fuel cells to wastewater treatment and energy production: a mini review, Sci. Total Environ., 639 (2018) 910–920.
[4] Z. Du, H. Li, T. Gu, A state of the art review on microbial fuel cells: a promising technology for wastewater treatment and bioenergy, Biotechnol. Adv., 25 (2007) 464–482.
[5] J. Lee, C.A. Ng, P.K. Lo, M.J.K. Bashir, Enhancement of renewable electrical energy recovery from palm oil mill effluent by microbial fuel cell with activated carbon, Energy Sources Part A, 41 (2019) 2662–2674.
[6] M. Li, M. Zhou, X. Tian, C. Tan, C.T. McDaniel, D.J. Hassett, T. Gu, Microbial fuel cell (MFC) power performance improvement through enhanced microbial electrogenicity, Biotechnol. Adv., 36 (2018) 1316–1327.
[7] A. Arkatkar, A.K. Mungray, P. Sharma, Effect of treatment on electron transfer mechanism in a microbial fuel cell, Energy Sources Part A, (2019) 1–16, doi: 10.1080/15567036.2019.1668878.
[8] S.N. Mohamed, T. Jayabalan, K. Muthukumar, Simultaneous bioenergy generation and carbon dioxide sequestration from food wastewater using algae microbial fuel cells, Energy Sources Part A, (2019) 1–9, doi: 10.1080/15567036.2019.1666932.
[9] D. Jothinathan, R.T. Wilson, Production of bioelectricity in MFC by *Pseudomonas fragi* DRR-2 (psychrophilic) isolated from goat rumen fluid, Energy Sources Part A, 39 (2017) 433–440.
[10] C. Santoro, C. Arbizzani, B. Erable, I. Ieropoulos, Microbial fuel cells: from fundamentals to applications. A review, J. Power Sources, 356 (2017) 225–244.
[11] V.S. Shrivastava, Int. J. Chem., Tech Research CODEN, USA, 4 (2012) 1038–1043.
[12] W. Xing, H.H. Ngo, S.H. Kim, W.S. Guo, P. Hagare, Adsorption and bioadsorption of granular activated carbon (GAC) for dissolved organic carbon (DOC) removal in wastewater, Bioresour. Technol., 99 (2008) 8674–8678.
[13] A.H. Ali, H.A. Al-Mussawy, M.J. Hussein, N.J. Hamadi, Comparison between conventional and modified microbial fuel cell for wastewater treatment and electricity generation, Int. J. Environ. Sci. Technol., 16 (2019) 8141–8150.
[14] N. Menek, Y. Karman, Polarographic and voltammetric investigation of 8-hydroxy-7-(4-sulfo-1naphthylazo)-5-quinoline sulfonic acid, Dyes Pigm. J., 67 (2005) 9–14.
[15] P.M. Alexander, I. Zayas, Particle size and shape effects on adsorption rate parameters, J. Environ. Eng., 115 (1989) 41–55.
[16] N. Ahalya, T.V. Ramachandra, R.D. Kanamadi, Biosorption of heavy metals, Res. J. Chem. Environ., 7 (2003) 71–78.
[17] H.R. Maier, G.C. Dandy, Neural networks for the prediction and forecasting of water resources variables: a review of modelling issues and applications, Environ. Modell. Software, 15 (2000) 101–123.
[18] V. Karthik, K. Saravanan, T. Thomas, M. Devi, Review on microbial decolorization of textile dyes, J. Chem. Pharm. Sci., 7 (2014) 293–300.
[19] S. Kannan, K. Dhandayuthapani, M. Sultana, Decolorization and degradation of azo due – Remazol Black B by newly isolated *Pseudomonas putida*, Int. J. Curr. Microbiol. Appl. Sci., 2 (2013) 108–116.
[20] X.-Y. Yong, J. Feng, Y.-L. Chen, D.-Y. Shi, Y.-S. Xu, J. Zhou, S.-Y. Wang, L. Xu, Y.-C. Yong, Y.-M. Sun, C.-L. Shi, P.-K. OuYang, T. Zheng, Enhancement of bioelectricity generation by cofactor manipulation in microbial fuel cell, Biosens. Bioelectron., 56 (2014) 19–25.
[21] H. Liu, R. Ramnarayanan, B.E. Logan, Production of electricity during wastewater treatment using a single chamber microbial fuel cell, Environ. Sci. Technol., 38 (2004) 2281–2285.
[22] A. Ramanavicius, A. Kausaite, A. Ramanaviciene, Enzymatic biofuel cell based on anode and cathode powered by ethanol, Biosens. Bioelectron., 24 (2008) 767–772.
[23] B. Min, S. Cheng, B.E. Logan, Electricity generation using membrane and salt bridge microbial fuel cells, Water Res., 39 (2005) 1675–1686.
[24] S.A. Patil, F. Harnisch, B. Kapadnis, U. Schröder, Electroactive mixed culture biofilms in microbial bioelectrochemical systems: the role of temperature for biofilm formation and performance, Biosens. Bioelectron., 26 (2010) 803–808.
[25] J. Yu, X. Wang, P. Yue, Optimal decolorization and kinetic modeling of synthetic dyes by *Pseudomonas* strains, Water Resour., 35 (2001) 3579–3585.
[26] E.Z. Gomaa, Biodegradation and detoxification of azo dyes by some bacterial strains, Microbiol. J., 6 (2016) 15–24.
[27] W. Miran, M. Nawaz, A. Kadam, S. Shin, J. Heo, J. Jang, D.S. Lee, Microbial community structure in a dual chamber microbial fuel cell fed with brewery waste for azo dye degradation and electricity generation, Environ. Sci. Pollut. Res., 22 (2015) 13477–13485.
[28] W.C. Tsan, C.W. Jung, H.R. Yao. Effect of culture time on the growth curve and power performance in a microbial fuel cell at a fixed amount of liquid culture, Int. J. Green Energy, 13 (2016) 695–702.
[29] J. Qu, Research progress of novel adsorption processes in water purification: a review, J. Environ. Sci., 20 (2008) 1–13.
[30] J.M. Mousa, A.H. Afaj, E. Abd-Alwahed, Study of removal of Pb, Zn, Cu and Ni ions from Iraqi factories wastewater using local porcelanite rocks, Iraqi Natl. J. Chem., 39 (2010) 445–454.
[31] J. Jayaprakash, A. Parthasarathy, R. Viraraghavan, Decolorization and degradation of monoazo and diazo dyes in *Pseudomonas* catalyzed microbial fuel cell, Environ. Prog. Sustainable Energy, 35 (2016) 1623–1628.
[32] H. Ding, Y. Li, A. Lu, S. Jin, C. Quan, C. Wang, X. Wang, C. Zeng, Y. Yan, Photocatalytically improved azo dye reduction in a microbial fuel cell with rutile-cathode, Bioresour. Technol., 101 (2010) 3500–3505.
[33] N.M. Mahdi, A.H. Ali, Study the relationship between bacterial growth, Congo red dye removal and voltage production using single chamber microbial fuel cell, J. Phys. Conf. Ser., 1895 (2021) 012041, doi: 10.1088/1742-6596/1895/1/012041.